The profile of the spinal column in subjects with lumbar developmental spinal stenosis

Authors: [1]Marcus Kin Long Lai (marcuslai1999@hotmail.com)
[1]Prudence Wing Hang Cheung, BDSc(Hons) (gnuehcp6@hotmail.com)
[2]Dino Samartzis, DSc (dino_samartzis@rush.edu)
[3]Jaro Karppinen, MD, PhD (jaro.karppinen@ttl.fi)
[1]Kenneth Man-Chee Cheung, MBBS, MD, FRCS, FHKCOS, FHKAM (cheungmc@hku.hk)
[1]Jason Pui Yin Cheung, MBBS, MMedSc, MS, PDipMDPath, MD, FHKCOS, FHKAM, FRCSEd (cheungjp@hku.hk)

Affiliations: [1]Department of Orthopaedics and Traumatology, The University of Hong Kong, Pokfulam, Hong Kong SAR, China
[2]Medical Research Center Oulu, Oulu University Hospital and University of Oulu, Oulu, Finland; Finnish Institute of Occupational Health, Oulu, Finland
[3]Department of Orthopedic Surgery, Rush University Medical Center, Chicago, Il, USA; International Spine Research and Innovation Initiative, RUSH University Medical Center, Chicago, IL, USA

Disclosure: The authors have no financial or competing interests to disclose.

Funding: Supported by the Master of Research in Medicine (MRes) programme at the University of Hong Kong, the Hong Kong Theme-Based Research Scheme (T12-708/12N), and AOSpine regional grant (Asia-Pacific).

Key Words: Lumbar; developmental spinal stenosis; magnetic resonance imaging; degenerative

Correspondence: **Jason Pui Yin Cheung**
Department of Orthopaedics & Traumatology
The University of Hong Kong
Professorial Block, 5th Floor
102 Pokfulam Road, Pokfulam
Hong Kong, SAR, China
Tel: (+852) 2255-4581
Fax: (+852) 2817-4392
Email: cheungjp@hku.hk

Role of each author: MKLL collected and interpreted the data, and wrote the manuscript. PWHC interpreted the data and edited the manuscript. DS acquired the images. Jaro Karppinen collected the data. KMCC acquired the images. JPYC designed and supervised the study, collected and interpreted the data, and wrote the manuscript. All authors confirmed authorship and approved the submission file.

The profile of the spinal column in subjects with lumbar developmental spinal stenosis

ABSTRACT

Aims

To determine the differences in spinal imaging phenotypes between subjects with and without DSS in a population-based cohort.

Patients and Methods

This was a radiological analysis of 2387 subjects who underwent L1-S1 magnetic resonance imaging (MRI). Means and ranges were calculated for their age, gender, body mass index (BMI) and MRI measurements. AP vertebral canal diameters were utilized to differentiate cases of DSS from controls. Other imaging parameters included the vertebral body dimensions, spinal canal dimensions, disc degeneration scores and facet joint orientation. Mann-Whitney *U* and chi-square tests were conducted to search for measurement differences between cases and controls. To identify possible associations between DSS and MRI parameters, parameters that were statistically significant in the univariate binary logistic regression were included in a multivariate stepwise logistic regression after adjusting for subject demographics.

Results

Axial AP vertebral canal diameter, interpedicular distance, AP dural sac diameter, lamina angle and sagittal mid-vertebral body height were significantly different between cases and controls

(all $p<0.05$). Narrower interpedicular distance and AP dural sac diameter were associated with DSS (OR 0.506-0.745; p=0.001-0.002). Lamina angle (OR 1.127; p=0.002) and right facet joint angulation (OR 0.022; p=0.002) were also associated with DSS. No association was observed between disc parameters and DSS.

Conclusion

From this large-scale cohort, the canal size is found to be independent of subject body habitus. Other than spinal canal dimensions, abnormal orientations of lamina angle and facet joint angulation may also be a result of developmental variations, leading to increased likelihood of DSS. Other skeletal parameters are spared. Besides, there is no relationship between DSS and soft tissue changes of the spinal column, which suggested DSS is a unique result of bony maldevelopment. Findings should be validated in other ethnicities and populations.

Keywords: Lumbar; developmental spinal stenosis; magnetic resonance imaging; degenerative

Level of Evidence: Type I diagnostic study

Clinical Relevance

- The vertebral canal size is independent of subject body habitus and vertebral body dimensions.
- A more obtuse lamina angle and smaller dural sac is associated with the presence of DSS.
- DSS is not associated with disc and endplate parameters including disc herniation, disc generation, Schmorl's nodes, endplate irregularity, high intensity zone lesions, and Modic changes.

INTRODUCTION

Lumbar developmental spinal stenosis (DSS) is likely a result of genetic disturbance during fetal and postnatal development of the lumbosacral spine[1-3]. It is of great clinical importance due to its high reoperation rate of up to 22%[4], and the presence of multilevel stenosis. Verbiest[5] proposed that patients with DSS have shorter laminae and as a result shorter anteroposterior (AP) lumbar canal diameters at multiple levels compared to non-DSS, due to its developmental nature. The pre-existing narrowed vertebral canal predisposes patients to a lower threshold of neural compression, in which a milder degree of degenerative changes of the lumbar spine is already sufficient to develop symptoms[6-15]. It was suggested that the canal size ceases to change beyond pubertal growth and skeletal maturity[16]. Such evidence provided additional confirmation to its genetic origin, with several genes identified to be closely associated with DSS, including the low-density lipoprotein receptor-related protein 5 (LRP5) that is a key component in the Wnt pathway for skeletal homeostasis.[12]

It is therefore clear that subjects with DSS have small canal sizes due to abnormal development of the lumbar spine. Current studies concentrate on defining the entity mainly with the vertebral canal size radiologically[7,11,17], but observing the changes of other radiological appearances of the spinal column is also necessary to indicate the degree of spinal dysplasia and its genetic origin. However, it is uncertain whether other specific osseous changes of the lumbar spinal column are presented concurrently in patients with a maldeveloped lumbar canal. Changes may be contributed by subjects' height, weight, body mass index (BMI) and vertebral size. Similar changes may also occur through altered development of the spinal column.

On the other hand, scattered articles proposed possible associations between DSS and soft tissue changes of the lumbar spine, but they were still controversial and preliminary, and their underlying mechanisms are not fully understood. Cheung *et al*[13] previously identified an

inverse relationship between lumbar vertebral canal size and the degree of ligamentum flavum fibrosis by utilizing standard magnetic resonance imaging (MRI). Another study by Soldatos *et al*[18] suggested a positive association between DSS and soft-tissue elements including annular tear, disc bulging and herniation. In contrast, Akar *et al*[19] found no relationship between canal size and facet joint angle and degree of facet tropism though their results should be cautioned due to small sample size. Changes in soft tissues around the canal such as disc herniation may further narrow the spinal canal with earlier onset of neurological compromise[16].

Therefore, to address our limited understanding of the association between DSS with different spinal tissues, we aim to determine the associations of DSS with osseous and soft tissue changes of the spinal column. We hypothesized that DSS is a result of maldevelopment rather than reflecting a small sized subject, and is associated with disc and facet joint changes. Thus, the aim of study is to determine the differences in various spinal imaging phenotypes between subjects with and without DSS in a population-based cohort.

PATIENTS AND METHODS

Study Design and Population

This was a cross-sectional study of 2387 subjects with axial and sagittal MRI available for measurements and data analysis. They were all participants of the Hong Kong Disc Degeneration Cohort Study[7,17,20-22], which was a southern Chinese population-based cohort openly recruited via newspaper advertisement, posters and e-mails regardless of their social and economic status. None of the subjects had prior spinal surgeries, spinal tumours and marked spinal deformities. The selection was not based on the presence or absence of clinical symptoms. However, whether they had any low back pain or radicular leg pain in the past month and year was recorded. All subjects underwent T1-weighted axial MRI and T2-weighted sagittal MRI of the lumbosacral spine (L1-S1)[23]. Informed consent was obtained for each

subject and ethics was approved by a local institutional review board. The demographics of the patient cohort is described in Table 1.

MRI Protocol

1.5 or 3T HD MRI machines were utilized for imaging. All subjects were in supine position. The following protocol was used for L1-S1 T1-weighted axial scans: Field of view of 21cm×21cm, slice thickness of 4mm, slice spacing of 0.4mm, and imaging matrix of 218×256. The following protocol was used for L1-S1 T2-weighted sagittal scans: Field of view of 28cm×28cm, slice thickness of 5mm, slice spacing of 1mm, and imaging matrix of 448×336. For T1- and T2-weighted MRI, the repetition time were 500ms-800ms and 3320ms respectively, while their echo time were 9.5ms and 85ms. 11 parallel slices were made at each spinal level with reference to the adjacent endplates.

Measurements

Measurements were taken by two individual investigators who were blinded to all demographical and clinical information. Consensus on obtaining the measurements were reached before the assessment. A total of 40 subjects were randomly selected by another independent investigator for repeated measurements in which the first and second round of measurements were at least 4 weeks apart. These measurements were used to calculate the intraobserver and interobserver reliability.

All measurements on the T1-weighted axial MRI utilized the cut with the thickest pedicle diameter that also included the vertebral body, pedicle and lamina (Figure 1). Measurements included midline AP vertebral body diameter, mid-vertebral body width, midline AP vertebral canal diameter, interpedicular distance, midline AP dural sac diameter, left and right pedicle width, lamina angle, and left and right facet joint angle at L1-S1. Lamina

angle (Figure 2) was the angle made by 2 lines extending from the junction where the pedicle joined the lamina to the base of the spinous process. Facet joint angle (Figure 3) was the angle made by the junction between a line joining the corners of the facet joint and the transverse plane. Facet joint angulation of less than 58º at L4-L5 was regarded as normal[24]. Facet joint tropism was noted if the difference between left facet joint angle and right facet joint angle was more than 8 degrees as reported by Samartzis *et al*[24].

T2-weighted sagittal MRI measurements were made on the midsagittal cut with the most prominent spinous process. Skeletal measurements included midline AP vertebral body diameter and mid-vertebral body height at L1-S1 (Figure 4). Disc measurements (Figure 5) included any disc herniation, Pfirrmann grading[25], Schmorl's node[26], endplate irregularity, high intensity zone (HIZ) lesions[27], Modic changes[28], and anterior marrow change. Disc herniation was further divided into 4 categories: 0 = no disc herniation; 1 = posterior disc bulging (disc is displaced beyond a virtual line connecting the posterior edges of two adjacent vertebrae); 2 = disc extrusion (distance between the edge of the protruded disc into the spinal canal was greater than the distance between edges of the base of the disc); 3 = disc sequestration[29-31]. Pfirrmann grading of disc degeneration with score 1-5 was utilized as previously published[25]: 1 = homogeneous bright white disc; 2 = inhomogeneous white disc ± horizontal bands; 3 = inhomogeneous grey disc; 4 = inhomogeneous grey to black disc; 5 = inhomogeneous black disc. The total disc herniation score and Pfirrmann grading were calculated by adding up their individual score per disc level. Schmorl's node was described as herniation of the nucleus pulposus into the adjacent vertebrae. Endplate irregularity was described as presence of an irregular surface at the endplates. HIZ was characterized by high-intensity area of the annulus fibrosus either posteriorly or anteriorly. Modic changes and anterior marrow changes were signal intensity changes at vertebral body adjacent to the

endplates. All MRI readings and measurements were conducted by Philips DICOM Viewer 3.0 (Philips, Andover, MA).

Definition of Lumbar Developmental Spinal Stenosis

The definition of DSS was established from those proposed by Cheung *et al*[7] by considering the significance of multilevel stenosis as patients with DSS often have multiple stenotic levels. Subjects with AP vertebral canal diameter below the proposed cutoffs in 3 or more levels were identified as abnormal. Three or more levels were decided because two stenotic levels are equivalent to three vertebral levels (e.g. L4, L5 and S1) when a multi-level decompression is required (L4-S1 decompression). After identifying the abnormal subjects, the new cutoff values were established by their level-specific median with the best sensitivity and specificity. Therefore, our definition of DSS (cases) was inclusion of 3 or more spinal levels (Table 2) with L1<19mm, L2<19mm, L3<18mm, L4<18mm, L5<18mm, S1<16mm. Otherwise, subjects were identified as controls.

Statistical Analysis

Subject demographics (age, gender, weight, height and BMI) were recorded at the time of the MRI, and their means, standard deviations and ranges were calculated. The means and ranges of the skeletal parameters were also calculated. For detecting differences between DSS and non-DSS subjects, Mann-Whitney *U* tests were performed for age, height, weight, BMI, T1-weighted axial MRI measurements, sagittal midline AP vertebral body diameter and sagittal mid-vertebral body height, while chi-square tests were used for gender and disc measurements. Intraobserver and interobserver reliability assessments were based on Cronbach α analysis. An α values of 0.90 to 1.00 was noted to have excellent reliability, while an α values of 0.80 to 0.89 was noted to have good reliability[32]. Excellent interobserver (α = 0.90 – 0.96) and

intraobserver reliability (α = 0.92 – 0.99 and α = 0.92 – 0.99) between the two independent investigators were noted from the measurements.

Univariate logistic regression analyses were conducted to detect any association between variables and the presence of DSS. Variables included all MRI measurements except the axial midline AP vertebral canal diameter, as it was used to differentiate subjects with DSS from subjects without DSS. Parameters that were statistically significant ($p<0.05$) in the univariate logistic regression analyses were identified and integrated into a multivariate logistic regression analysis which was controlled for gender, age and BMI. Stepwise regression was run to establish both models as this was an exploratory research, and we were uncertain which variable would create the best prediction equations. Odds ratios (ORs) were reported. A P-value of less than 0.05 was considered as statistically significant and 95% confidence intervals (CIs) were reported. All statistical analyses were performed by SPSS Statistics 26 (IBM SPSS Inc., Chicago, Illinois).

RESULTS

From 2387 subjects, 7.2% (n=173) was identified to have DSS. The means, ranges and counts of all imaging parameters are presented in table 3. Subjects with DSS had shorter axial vertebral canal diameter, interpedicular distance, AP dural sac diameter and vertebral body height at L1-S1. Besides, subjects with DSS had higher disc herniation scores, higher disc degeneration scores and larger right facet joint angulation. No association was observed between DSS and BMI (p=0.195). After conducting the univariate logistic regression analyses (Table 4), parameters including axial AP vertebral body width, interpedicular distance, AP dural sac diameter, sagittal vertebral body height, lamina angle and right facet joint angulation were found to be significant factors associated with DSS and were integrated into the multivariate logistic regression model.

After adjusting for age, gender and BMI, the multivariate logistic regression model (Table 5) reached statistical significance (chi-square (9, n=2387) = 94.621; p<0.001). It correctly predicted 92.4% of the dichotomous DSS outcome. There were associations between DSS and interpedicular distance (OR 0.745; p=0.002; 95% CI: 0.618-0.900), AP dural sac diameter (OR 0.506; p<0.001; 95% CI: 0.400-0.641), lamina angle (OR 1.127; p=0.002; 95% CI: 1.045-1.214) and right facet joint angulation (OR 0.022; p=0.002; 95% CI: 0.002-0.247). Hence, besides the lamina angle which was more obtuse in patients with DSS, smaller interpedicular distance, AP dural sac diameter and right facet joint angulation had increased odds of DSS. No associations were observed with axial vertebral body width (OR 0.973; p=0.645; 95% CI: 0.865-1.094) and sagittal vertebral body height (OR 0.949; p=0.588; 95% CI: 0.785-1.147). If the significant factors were removed from the model, their effects were shown by the changes in -2 log likelihood in table 5.

DISCUSSION

DSS is a distinct pathology that can be appreciated radiologically, especially described on axial images[7]. With abnormally short laminae and small canal sizes at multiple levels, neural compression develops at a lower threshold and becomes symptomatic at an earlier age compared to patients with degenerative stenosis alone. Researchers suggest this stenotic nature to be developmental in origin as canal size only changes before and during pubertal growth[16]. It appears as if patients with DSS may be more prone to developing radicular leg symptoms. Currently, it is uncertain whether other radiological appearances of the spinal column are present and associated with the smaller vertebral canal. Our study, however, is the largest study that identify these relationships by utilizing multivariate regression analysis. We observed that subjects with DSS had smaller interpedicular distance and dural sac diameter. These subjects also have altered lamina angle and facet joint angles indicating different biomechanics exist

for the development of these spinal structures when compared to other elements of the spinal column. These findings are found to be independent of body size and the dimension of the vertebral body on axial and sagittal plane.

Subjects with DSS were not found to have a shorter height and lower weight compared to controls, as no significant associations were identified between BMI and vertebral dimensions with DSS. The results confirmed our hypothesis that DSS is likely a result of bony malformation of the spinal canal rather than due to the small size of subjects. Although BMI is not a sensitive indicator that reflects the body size of a person as it is affected by numerous environmental and physiological factors, this is one of the commonest and most convenient parameters that estimate the size of the subject. Our findings are reiterated by a similar but smaller study in which there was no relationship between spinal canal cross-sectional area with age and BMI[33]. Other than BMI, more sensitive indicators of the body size including the vertebral body dimensions were used in this study to assess their associations with DSS. Their insignificant associations provide stronger evidence which further justifies DSS as a pathology that confines to the morphology of the spinal canal.

It was also observed that the AP dural sac diameter were inversely associated with the presence of DSS, which suggests subjects with DSS have an increased likelihood of having a smaller sized thecal sac. The dural sac is a layer of thick membrane made of dense irregular connective tissue that is subject to variations. The spinal canal confines the size of the dural sac and thus dictates the amount of spinal stenosis needed to cause a significant compression. Our findings have several potential implications. Firstly, the size and morphology of the dural sac cross-sectional area has been shown to influence when intervention is required and the expected surgical outcomes.[34,35] In DSS with a naturally smaller sized thecal sac, the degree of cerebrospinal fluid to rootlet ration may be disproportionate to the severity of spinal stenosis. This leads to difficulties in interpreting the degree of neural tissue impingement. Secondly, the

success of indirect decompression of a spinal canal may rely on the increased size of dural sac cross-sectional area.[36] There may also be considerations when risk profiling for complications and their remediation steps.[37] With DSS, the space available for the dural sac to expand may be limited and may lead to variable outcomes. Whether this theory holds true requires further investigation.

Maldevelopment of the vertebral canal leading to pre-existing narrowing is a clinical concern for early neurological compromise. The defect is localized to the vertebral canal and thus is less likely to be a defect during embryonic development of the mesenchymal cells and sclerotomes, as some regions of the spinal column are well preserved. The development of parts of the spinal canal appear to be independent from the rest of the spinal column. DSS should therefore be listed as one of the major differential diagnoses when a patient presents with compressive symptoms. Interestingly, the lamina angle was associated with DSS, albeit not very impactful as seen by the small OR variations. Nevertheless, the appearance of the lamina may determine the shape of the canal depending on its angle. Anatomically, subjects with a more obtuse lamina angle should have a wider interpedicular distance and shorter AP vertebral canal diameter. These subjects are hence more susceptible to having DSS. Abnormal development of the articular processes of adjacent vertebrae can also affect the orientation of facet joint angulation. Although the right facet joint opening angle was associated with DSS, our results only reflect a unilateral association and are limited by the very small amount of abnormal cases. Therefore, this relationship may be spurious and has limited clinical implications.

Other than osseous changes of the lumbar spine, the relationship of DSS with the disc and disc-vertebral junction is also important[13,18,19]. Although a theory of concurrent DSS and early disc degeneration has been proposed[38,39], we found no such association in this study. This is, interestingly, a contradictory result compared to Soldatos *et al*[18] (n=100) and Akar *et al*[19]

(n=100), in which the former found positive relationship between DSS and disc herniation, while the latter found no relationship between DSS and facet joint angles or facet tropism. However, both studies are limited by their small sample sizes. Embryonically, the spinal column and the disc are originated from sclerotome and notochord respectively. It is possible that certain genetic factors only disrupt the process of canal development leading to bony dysplasia, but not the notochord and vertebral body. Although DSS and disc changes can coexist on the same patient, there is no evidence for more disc degeneration in patients with DSS which rejected our hypothesis. Furthermore, as observed from the symptomatology, there are no differences in prevalence of low back pain between patients with or without DSS. There may be uncertainties to where pain can arise.[40]

It is inevitable that there are limitations in the study. Firstly, we only utilized Chinese subjects which may limit the generalisability of the study. However, this reduces the variations between individuals for higher internal validity. Nevertheless, the results should be validated in another ethnicity and population. Secondly, as the subjects were openly recruited, we cannot control the number of males and females, which lead to imbalanced gender distribution and uncontrolled selection bias. Thirdly, due to the open recruitment, our findings may not fully reflect the true population. Fourthly, despite not including marked spinal deformities, a mild scoliosis may affect the orientation of the posterior element leading to discrepancies in lamina angle and facet joint angulation measurements. Fifth, our measurements were performed on subjects in supine position for MRIs. Whether imaging features change with posture remains to be studied. The use of 1.5T and 3T MRI may cause interpretation variances for disc degeneration and Pfirrmann grading as these depend on the disc intensity signals. One other important limitation is the use of MRIs for the study of DSS and other bony phenotypes. Computed tomography (CT) is the preferred study for the bony architecture. However, we chose to use an inferior imaging method with the MRI because it is more clinically practical.

MRIs are commonly available for study of patients undergoing spine surgery and it also avoids the radiation risks of CT to this population cohort. Furthermore, it is useful for our study of relationships with soft tissues like the intervertebral disc and thecal sac.

This is a large-scale study that examines the relationship of DSS with osseous and soft tissue elements of the lumbosacral spine under MRI. This study builds significantly upon the work of Cheung *et al*[7] with a large-scale population-based cohort as compared to patients who underwent surgery for lumbar spinal stenosis. In addition, a more structured and diagnostic criteria for multi-level DSS has been elucidated and can be used as a reference when planning surgery for a patient with lumbar spinal stenosis. Patients with DSS are more likely to have radicular leg pain which as compared to low back pain is more relevant to a patient with potential neural compression. This has significant clinical implications to patient quality of life and their risk of developing clinically significant disease that require interventions. With these benchmarks, surgeons should consider pre-emptive decompression surgery at levels with DSS to prevent adjacent level reoperations.[4] Importantly, this study suggests that other than a pre-existing narrowed vertebral canal, the orientation of the lamina angle and the facet joint angulation are also associated with DSS. It has no associations with other bony and soft tissue parameters of the spinal column. This entity is likely a result of maldevelopment of the spinal canal. Its underlying molecular processes may be independent from other components of the spinal column. Future studies should demonstrate similar relationships between DSS and other radiological appearances in other ethnic cohorts. Also, as suggested by its strong developmental nature, the genetic origins and pathomechanisms of this maldevelopment should be a direction for further investigation.

REFERENCES

1. **Kirkaldy-Willis WH, Wedge JH, Yong-Hing K, Reilly J.** Pathology and pathogenesis of lumbar spondylosis and stenosis. *Spine (Phila Pa 1976)* 1978;3:319-328.
2. **Verbiest H.** Further experiences on the pathological influence of a developmental narrowness of the bony lumbar vertebral canal. *J Bone Joint Surg Br* 1955;37-B(4):576-583.
3. **Verbiest H.** Fallacies of the present definition, nomenclature, and classification of the stenoses of the lumbar vertebral canal. *Spine (Phila Pa 1976)* 1976;1:217-225.
4. **Cheung PWH, Fong HK, Wong CS, Cheung JPY.** The influence of developmental spinal stenosis on the risk of re-operation on an adjacent segment after decompression-only surgery for lumbar spinal stenosis. *Bone Joint J* 2019;101-B:154-161.
5. **Verbiest H.** A radicular syndrome from developmental narrowing of the lumbar vertebral canal. *J Bone Joint Surg Br* 1954;36-B:230-237.
6. **Chatha DS, Schweitzer ME.** MRI criteria of developmental lumbar spinal stenosis revisited. *Bulletin of the NYU hospital for joint diseases* 2011;69:303-307.
7. **Cheung JP, Samartzis D, Shigematsu H, Cheung KM.** Defining clinically relevant values for developmental spinal stenosis: a large-scale magnetic resonance imaging study. *Spine (Phila Pa 1976)* 2014;39:1067-1076.
8. **Eisenstein S.** Lumbar vertebral canal morphometry for computerised tomography in spinal stenosis. *Spine (Phila Pa 1976)* 1983;8:187-191.
9. **Postacchini F, Pezzeri G, Montanaro A, Natali G.** Computerised tomography in lumbar stenosis. A preliminary report. *J Bone Joint Surg Br* 1980;62-B:78-82.

10. **Singh K, Samartzis D, Vaccaro AR, et al.** Congenital lumbar spinal stenosis: a prospective, control-matched, cohort radiographic analysis. *The spine journal : official journal of the North American Spine Society* 2005;5:615-622.
11. **Kitab SA, Alsulaiman AM, Benzel EC.** Anatomic radiological variations in developmental lumbar spinal stenosis: a prospective, control-matched comparative analysis. *The spine journal : official journal of the North American Spine Society* 2014;14:808-815.
12. **Cheung JPY, Yiu K, Kwan K, Cheung KMC.** Mean 6-Year Follow-up of Magnetically Controlled Growing Rod Patients With Early Onset Scoliosis: A Glimpse of What Happens to Graduates. *Neurosurgery* 2018.
13. **Cheung PWH, Tam V, Leung VYL, et al.** The paradoxical relationship between ligamentum flavum hypertrophy and developmental lumbar spinal stenosis. *Scoliosis Spinal Disord* 2016;11:26.
14. **Postacchini F, Pezzeri G.** CT scanning versus myelography in the diagnosis of lumbar stenosis. A preliminary report. *Int Orthop* 1981;5:209-215.
15. **Lai MKL, Cheung PWH, Cheung JPY.** A systematic review of developmental lumbar spinal stenosis. *Eur Spine J* 2020.
16. **Kim KH, Park JY, Kuh SU, Chin DK, Kim KS, Cho YE.** Changes in spinal canal diameter and vertebral body height with age. *Yonsei Med J* 2013;54:1498-1504.
17. **Cheung JPY, Ng KKM, Cheung PWH, Samartzis D, Cheung KMC.** Radiographic indices for lumbar developmental spinal stenosis. *Scoliosis Spinal Disord* 2017;12:3.
18. **Soldatos T, Chalian M, Thawait S, et al.** Spectrum of magnetic resonance imaging findings in congenital lumbar spinal stenosis. *World J Clin Cases* 2014;2:883-887.
19. **Akar E, Somay H.** Comparative morphometric analysis of congenital and acquired lumbar spinal stenosis. *J Clin Neurosci* 2019;68:256-261.

20. **Cheung KM, Samartzis D, Karppinen J, Luk KD.** Are "patterns" of lumbar disc degeneration associated with low back pain?: new insights based on skipped level disc pathology. *Spine (Phila Pa 1976)* 2012;37:E430-438.

21. **Mok FP, Samartzis D, Karppinen J, Luk KD, Fong DY, Cheung KM.** ISSLS prize winner: prevalence, determinants, and association of Schmorl nodes of the lumbar spine with disc degeneration: a population-based study of 2449 individuals. *Spine (Phila Pa 1976)* 2010;35:1944-1952.

22. **Samartzis D, Karppinen J, Chan D, Luk KD, Cheung KM.** The association of lumbar intervertebral disc degeneration on magnetic resonance imaging with body mass index in overweight and obese adults: a population-based study. *Arthritis Rheum* 2012;64:1488-1496.

23. **Cheung JP, Shigematsu H, Cheung KM.** Verification of measurements of lumbar spinal dimensions in T1- and T2-weighted magnetic resonance imaging sequences. *Spine J* 2014;14:1476-1483.

24. **Samartzis D, Cheung JP, Rajasekaran S, et al.** Critical Values of Facet Joint Angulation and Tropism in the Development of Lumbar Degenerative Spondylolisthesis: An International, Large-Scale Multicenter Study by the AOSpine Asia Pacific Research Collaboration Consortium. *Global Spine J* 2016;6:414-421.

25. **Pfirrmann CW, Metzdorf A, Zanetti M, Hodler J, Boos N.** Magnetic resonance classification of lumbar intervertebral disc degeneration. *Spine (Phila Pa 1976)* 2001;26:1873-1878.

26. **Kyere KA, Than KD, Wang AC, et al.** Schmorl's nodes. *Eur Spine J* 2012;21:2115-2121.

27. **Aprill C, Bogduk N.** High-intensity zone: a diagnostic sign of painful lumbar disc on magnetic resonance imaging. *Br J Radiol* 1992;65:361-369.

28. **Modic MT, Steinberg PM, Ross JS, Masaryk TJ, Carter JR.** Degenerative disk disease: assessment of changes in vertebral body marrow with MR imaging. *Radiology* 1988;166:193-199.

29. **Cheung KM, Karppinen J, Chan D, et al.** Prevalence and pattern of lumbar magnetic resonance imaging changes in a population study of one thousand forty-three individuals. *Spine (Phila Pa 1976)* 2009;34:934-940.

30. **Maatta JH, Karppinen JI, Luk KD, Cheung KM, Samartzis D.** Phenotype profiling of Modic changes of the lumbar spine and its association with other MRI phenotypes: a large-scale population-based study. *The spine journal : official journal of the North American Spine Society* 2015;15:1933-1942.

31. **Teraguchi M, Cheung JPY, Karppinen J, et al.** Lumbar high-intensity zones on MRI: imaging biomarkers for severe, prolonged low back pain and sciatica in a population-based cohort. *Spine J* 2020;20:1025-1034.

32. **Vangeneugden T, Laenen A, Geys H, Renard D, Molenberghs G.** Applying concepts of generalizability theory on clinical trial data to investigate sources of variation and their impact on reliability. *Biometrics* 2005;61:295-304.

33. **Griffith JF, Huang J, Law SW, et al.** Population reference range for developmental lumbar spinal canal size. *Quant Imaging Med Surg* 2016;6:671-679.

34. **Mannion AF, Fekete TF, Pacifico D, et al.** Dural sac cross-sectional area and morphological grade show significant associations with patient-rated outcome of surgery for lumbar central spinal stenosis. *Eur Spine J* 2017;26:2552-2564.

35. **Schizas C, Theumann N, Burn A, et al.** Qualitative grading of severity of lumbar spinal stenosis based on the morphology of the dural sac on magnetic resonance images. *Spine (Phila Pa 1976)* 2010;35:1919-1924.

36. **Nakashima H, Kanemura T, Satake K, et al.** Indirect Decompression on MRI Chronologically Progresses After Immediate Postlateral Lumbar Interbody Fusion: The Results From a Minimum of 2 Years Follow-Up. *Spine (Phila Pa 1976)* 2019;44:E1411-E1418.

37. **Takenaka S, Makino T, Sakai Y, et al.** Prognostic impact of intra- and postoperative management of dural tear on postoperative complications in primary degenerative lumbar diseases. *Bone Joint J* 2019;101-B:1115-1121.

38. **Kitab S, Habboub G, Abdulkareem SB, Alimidhatti MB, Benzel E.** Redefining lumbar spinal stenosis as a developmental syndrome: does age matter? *J Neurosurg Spine* 2019;31:357-365.

39. **Kitab S, Lee BS, Benzel EC.** Redefining lumbar spinal stenosis as a developmental syndrome: an MRI-based multivariate analysis of findings in 709 patients throughout the 16- to 82-year age spectrum. *J Neurosurg Spine* 2018;29:654-660.

40. **Liu N, Goodman SB, Lachiewicz PF, Wood KB.** Hip or spine surgery first?: a survey of treatment order for patients with concurrent degenerative hip and spinal disorders. *Bone Joint J* 2019;101-B:37-44.

Table 1: Associations of Lumbar Developmental Spinal Stenosis with Subjects' Demographics

	DSS Mean	Non-DSS Mean	P-value
Number of Subjects	n=173	n=2214	
Age, *years* (range)	52.5 (22.9 – 75.8)	51.1 (16.7 – 86.3)	0.102
Gender, *N* (%)			
Male	55 (31.8%)	860 (38.8%)	0.068
Female	118 (68.2%)	1354 (61.2%)	
Weight, *kg* (range)	61.9 (38.5 – 91.5)	61.9 (33.2 – 111.1)	0.903
Height, *m* (range)	1.62 (1.45 – 1.85)	1.62 (1.25 – 1.91)	0.787
BMI, kg/m^2 (range)	23.4 (17.1 – 30.1)	23.6 (14.2 – 39.7)	0.700
LBP in the past month	92 (53.2%)	1159 (52.3%)	0.351
LBP in the past year	120 (69.4%)	1470 (66.4%)	0.069
Radicular leg pain in the past month	61 (35.3%)	611 (27.6%)	0.008
Radicular leg pain in the past year	83 (48.0%)	821 (37.1%)	0.001
DSS: developmental spinal stenosis; BMI: body mass index; LBP: low back pain.			

Table 2: Radiological Definition of Developmental Spinal Stenosis

Vertebral Level	Radiological Cutoff
L1	19mm
L2	19mm
L3	18mm
L4	18mm
L5	18mm
S1	16mm

Requires 3 or more levels with measurements under the above cut-off of the anteroposterior vertebral canal diameter

1 Table 3: Measurements of all imaging phenotypes

	Cases (DSS)	Controls	P-Value
Number of subjects	n=173	n=2214	
Mean Axial Anteroposterior Vertebral Canal Diameter, *mm* (range)			
L1	19.4 (16.7-22.0)	21.3 (17.2-29.6)	<0.001*
L2	18.8 (15.3-22.7)	21.0 (16.7-30.2)	<0.001*
L3	18.1 (14.7-22.4)	20.5 (15.5-29.7)	<0.001*
L4	17.5 (14.9-21.4)	20.3 (14.1-28.9)	<0.001*
L5	17.3 (14.1-24.4)	20.3 (12.7-32.3)	<0.001*
S1	16.1 (11.2-21.4)	18.8 (9.4-30.3)	<0.001*
Mean Axial Midline Anteroposterior Vertebral Body Diameter, *mm* (range)			
L1	25.6 (20.9-32.8)	25.8 (18.5-39.1)	0.282
L2	27.1 (21.1-34.0)	27.1 (19.5-37.7)	0.870
L3	28.5 (22.2-36.9)	28.6 (20.2-39.5)	0.672
L4	28.8 (23.4-35.5)	28.8 (16.4-40.1)	0.987
L5	29.0 (20.5-37.1)	29.2 (20.2-42.3)	0.472
S1	27.2 (15.4-37.6)	27.8 (12.6-38.8)	0.133
Mean Axial Mid-Vertebral Body Width, *mm* (range)			
L1	34.3 (23.7-43.9)	35.0 (23.9-47.9)	0.025*
L2	35.4 (29.2-43.4)	36.2 (24.6-48.2)	0.010*
L3	36.9 (29.7-47.1)	37.4 (25.2-51.3)	0.072
L4	39.0 (31.7-47.7)	39.6 (17.8-59.2)	0.046*
L5	44.1 (33.9-56.6)	44.7 (20.3-60.5)	0.094
S1	49.3 (10.0-62.9)	51.6 (16.2-69.4)	<0.001*
Mean Interpedicular Distance, *mm* (range)			
L1	23.0 (19.3-28.5)	24.4 (16.6-35.5)	<0.001*
L2	23.5 (18.6-27.4)	24.7 (19.4-35.9)	<0.001*
L3	24.3 (11.0-33.2)	25.8 (19.8-37.7)	<0.001*
L4	26.0 (18.6-34.1)	27.4 (19.2-38.8)	<0.001*
L5	31.1 (22.8-39.9)	32.0 (20.5-47.4)	<0.001*
S1	33.3 (20.4-40.0)	35.6 (25.1-47.7)	<0.001*
Mean Anteroposterior Dural Sac Diameter, *mm* (range)			
L1	12.3 (9.1-15.7)	13.8 (8.2-22.5)	<0.001*
L2	11.4 (7.3-14.8)	13.1 (8.9-22.5)	<0.001*
L3	10.5 (6.0-23.2)	12.3 (5.8-25.0)	<0.001*
L4	9.4 (5.3-15.7)	11.4 (4.8-28.9)	<0.001*
L5	9.3 (5.4-15.5)	11.5 (4.27-32.5)	<0.001*
S1	8.0 (3.1-17.4)	10.1 (3.2-29.8)	<0.001*
Mean Right Pedicle Width, *mm* (range)			
L1	4.6 (1.6-9.4)	4.3 (0.8-11.2)	0.006*
L2	5.1 (2.0-9.3)	4.8 (1.2-11.5)	0.002*
L3	6.8 (2.9-11.4)	6.3 (2.0-12.4)	0.002*
L4	8.9 (4.0-14.6)	8.5 (2.7-18.9)	0.011*
L5	12.7 (5.6-23.4)	12.7 (6.1-22.3)	0.999
S1	17.6 (10.3-23.1)	17.6 (9.1-27.3)	0.941
Mean Left Pedicle Width, *mm* (range)			

L1	4.6 (1.8-10.1)	4.3 (0.6-11.2)	0.003*
L2	5.1 (2.4-9.1)	4.8 (1.0-10.5)	0.007*
L3	6.6 (3.0-12.8)	6.2 (1.4-12.9)	0.002*
L4	8.6 (3.7-14.9)	8.4 (3.2-27.2)	0.039*
L5	12.5 (5.6-20.9)	12.6 (6.5-27.5)	0.992
S1	17.6 (9.8-29.0)	17.7 (8.5-29.4)	0.714
Mean Lamina Angle, º (range)			
L1	121.0 (112.9-131.1)	119.3 (101.2-133.9)	<0.001*
L2	121.5 (110.4-131.4)	120.0 (102.9-134.9)	<0.001*
L3	121.9 (105.7-138.5)	120.0 (99.1-137.8)	<0.001*
L4	114.5 (99.2-132.7)	111.8 (88.9-128.0)	<0.001*
L5	103.5 (84.5-116.9)	100.7 (74.5-118.8)	<0.001*
S1	93.7 (70.9-109.4)	94.1 (65.8-111.3)	0.436
Mean Right Facet Joint Angle, º (range)			
L1/L2	57.0 (38.5-69.2)	56.2 (35.4-74.7)	0.046*
L2/L3	53.6 (31.6-68.4)	53.0 (31.8-69.4)	0.155
L3/L4	47.1 (31.0-65.9)	46.2 (23.7-65.6)	0.153
L4/L5	40.9 (25.4-62.1)	38.2 (16.1-61.0)	<0.001*
L5/S1	35.6 (14.3-54.2)	34.1 (12.8-62.9)	0.004*
Mean Left Facet Joint Angle, º (range)			
L1-L2	57.9 (38.8-71.7)	57.0 (38.1-72.7)	0.062
L2-L3	54.5 (34.3-70.6)	53.8 (33.1-72.7)	0.085
L3-L4	48.1 (30.1-65.0)	46.6 (24.7-67.5)	0.004*
L4-L5	41.9 (27.7-59.3)	38.9 (12.0-60.1)	<0.001*
L5-S1	36.4 (18.0-58.6)	34.7 (10.5-60.0)	0.003*
Mean Sagittal Midline Anteroposterior Vertebral Body Diameter, *mm* (range)			
L1	25.8 (19.2-36.8)	25.8 (18.4-42.5)	0.998
L2	27.0 (19.9-38.0)	26.8 (18.1-46.0)	0.410
L3	28.8 (21.7-40.0)	28.4 (19.7-46.2)	0.063
L4	29.4 (23.8-38.6)	29.1 (19.1-46.2)	0.293
L5	28.8 (21.4-39.8)	28.8 (19.2-46.1)	0.799
S1	21.6 (15.9-29.0)	22.3 (13.7-35.1)	0.005*
Mean Sagittal Mid-vertebral Body Height, *mm* (range)			
L1	22.7 (18.7-26.8)	23.1 (13.7-36.8)	0.005*
L2	23.4 (19.9-28.5)	23.8 (15.4-37.2)	0.005*
L3	23.4 (19.0-28.5)	23.8 (16.6-36.13)	0.003*
L4	22.8 (17.8-34.3)	23.4 (16.7-33.8)	<0.001*
L5	22.4 (17.6-29.1)	22.9 (15.0-33.7)	<0.001*
S1	24.9 (17.9-29.8)	25.7 (18.9-40.4)	<0.001*
Vertebral Disc and Endplate-Related Parameters			
Mean Disc Herniation Score (range)	2.5 (0.0-10.0)	2.1 (0.0-12.0)	0.010*
Mean Disc Degeneration Score (range)	15.5 (0.0-21.0)	14.8 (0.0-23.0)	0.002*
Schmorl's Nodes, *N* (%)	24 (13.9%)	294 (13.3%)	0.830
Endplate Irregularity, *N* (%)	45 (26.0%)	475 (21.5%)	0.163

High Intensity Zone, *N* (%)	58 (33.5%)	733 (33.1%)	0.914
Modic Change, *N* (%)	41 (23.7%)	490 (22.1%)	0.635
Anterior Marrow Change, *N* (%)	32 (18.5%)	387 (17.5%)	0.739
Right Facet Joint Angulation (ref: abnormal), *N* (%)	171 (98.8%)	2211 (99.9%)	0.005*
Left Facet Joint Angulation (ref: abnormal), *N* (%)	172 (99.4%)	2211 (99.9%)	0.168
Facet Joint Tropism, *N* (%)	47 (27.2%)	592 (26.7%)	0.902
**Statistically significant at 0.05 level*; DSS: developmental spinal stenosis			

1
2

Table 4: Univariate Binary Logistic Regression for Association between Independent Variables and DSS

Imaging Parameters	Chi-square Value	Accuracy of Prediction (% correct)	Odds Ratio (95% CI)	P-value
Age	19.205	92.8	1.017 (1.010-1.024)	<0.001*
Gender (ref: male)	82.600	92.8	1.898 (1.643-2.192)	<0.001*
BMI	26.263	92.7	1.020 (0.990-1.050)	0.195
Axial AP Vertebral Body Diameter	2.523	92.7	0.984 (0.965-1.004)	0.112
Axial Vertebral Body Width	15.541	92.7	0.981 (0.972-0.991)	<0.001*
Axial Interpedicular Distance	87.950	92.7	0.933 (0.919-0.947)	<0.001*
Axial AP Dural Sac Diameter	605.934	92.7	0.721 (0.692-0.732)	<0.001*
Axial Right Pedicle Width	2.469	92.7	1.010 (0.998-1.023)	0.116
Axial Left Pedicle Width	1.429	92.7	1.008 (0.995-1.020)	0.232
Sagittal Vertebral Body Diameter	0.106	92.8	1.003 (0.986-1.020)	0.744
Sagittal Vertebral Body Height	59.471	92.8	0.888 (0.861-0.916)	<0.001*
Lamina Angle	21.626	92.7	1.014 (1.008-1.020)	<0.001*
Disc Herniation	2.812	92.8	1.326 (0.953-1.844)	0.094
Disc Degeneration	0.315	92.8	1.028 (0.934-1.131)	0.574
Schmorl's Nodes	0.057	92.8	1.056 (0.675-1.653)	0.812
Endplate Irregularity	1.866	92.8	1.280 (0.898-1.825)	0.172
High Intensity Zone	0.013	92.8	1.019 (0.734-1.414)	0.910
Marrow Change	0.202	92.8	1.087 (0.755-1.565)	0.653
Anterior Marrow Change	0.095	92.8	1.065 (0.714-1.587)	0.758
Right Facet Joint Angulation (ref: abnormal)	8.194	92.7	0.115 (0.019-0.694)	0.018*
Left Facet Joint Angulation (ref: abnormal)	1.462	92.7	0.232 (0.024-2.242)	0.207
Facet Joint Tropism	2.777	92.7	0.727 (0.499-1.058)	0.096
**Statistically significant at 0.05 level and included in the multivariate binary logistic regression.* CI, confidence interval; BMI, body mass index; AP, anteroposterior.				

Table 5: Multivariate Stepwise Logistic Regression Analysis of the Association of DSS with Imaging Parameters

MRI Predictors	Regression Coefficient	Wald Chi-square	P-values	Odds ratio	95% CI	Change in -2 log likelihood
Age	-0.013	0.515	0.473	0.987	0.953-0.736	N/A
Gender (reference: male)	0.508	1.494	0.222	1.662	0.736-3.752	N/A
BMI	0.019	0.200	0.655	1.019	0.939-1.105	N/A
Axial Vertebral Body Width	-0.028	0.213	0.645	0.973	0.865-1.094	0.214
Interpedicular Distance	-0.294	9.379	0.002*	0.745	0.618-0.900	10.025*
AP Dural Sac Diameter	-0.681	31.911	<0.001*	0.506	0.400-0.641	35.361*
Sagittal Vertebral Body Height	-0.052	0.294	0.588	0.949	0.785-1.147	0.296
Lamina Angle	0.119	9.749	0.002*	1.127	1.045-1.214	10.112*
Right Facet Joint Angulation (ref: abnormal)	-3.819	9.570	0.002*	0.022	0.002-0.247	7.484*

**Statistically significant at 0.05 level.*
CI, confidence interval; N/A, not available; BMI, body mass index; AP, anteroposterior.

FIGURE LEGENDS

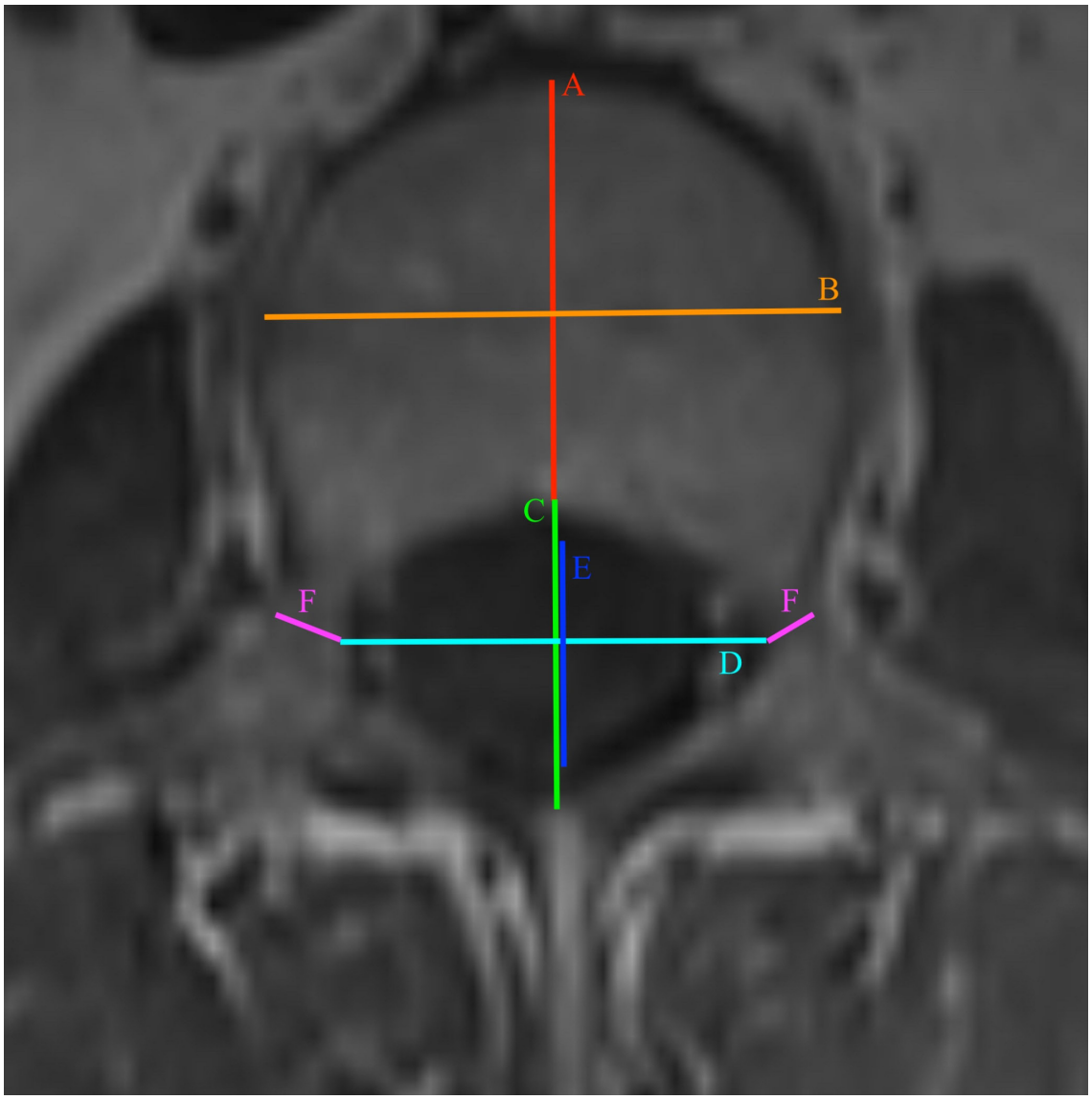

Figure 1: Axial magnetic resonance imaging measurements: (A) anteroposterior (AP) vertebral body diameter; (B) mid-vertebral body width; (C) midline AP vertebral canal diameter; (D) interpedicular distance; (E) midline AP dural sac diameter; (F) left and right pedicle width.

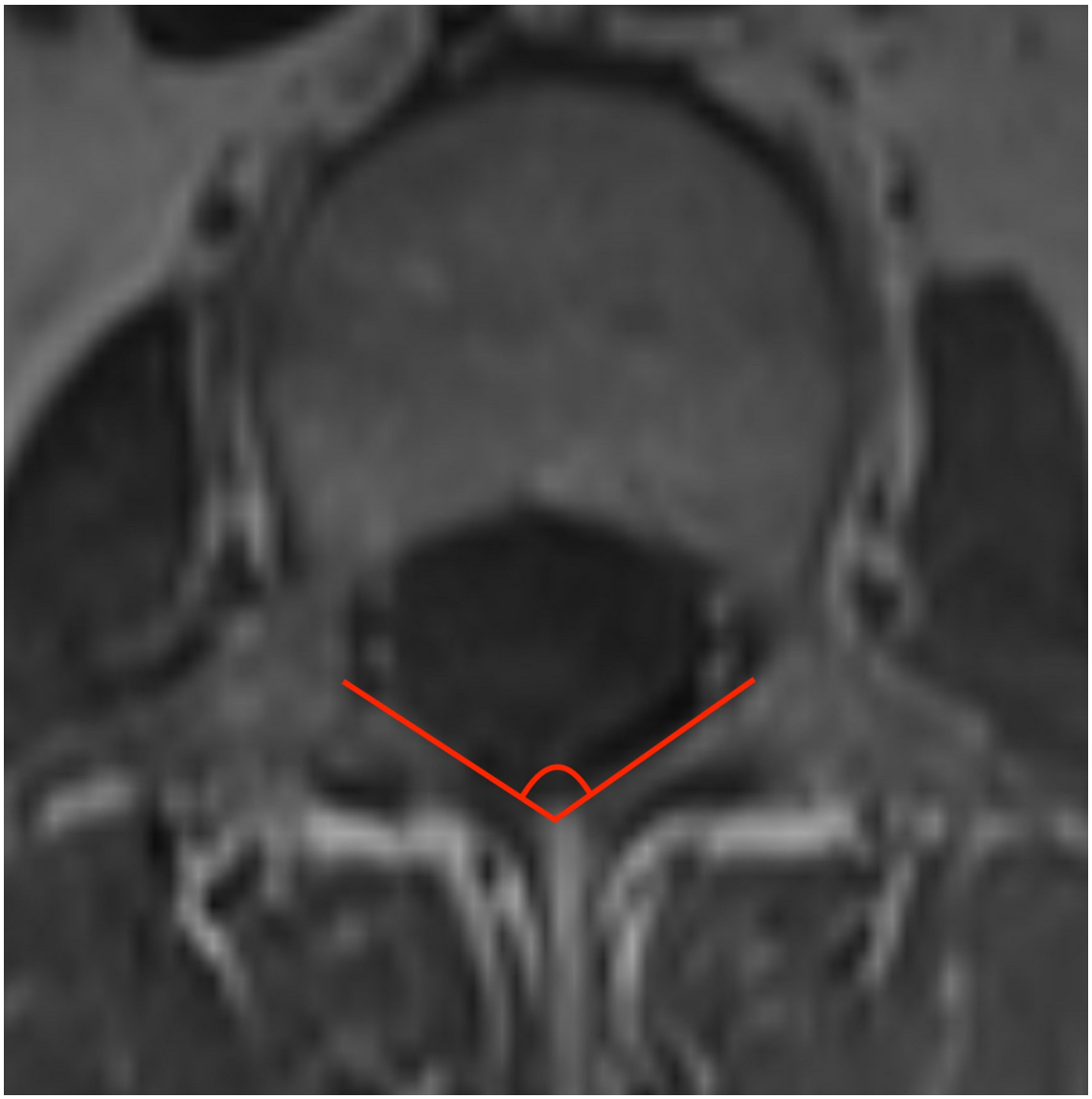

Figure 2: Axial magnetic resonance imaging measurement of the lamina angle (made by 2 lines extending from the junction where the pedicle joined the lamina to the base of the spinous process).

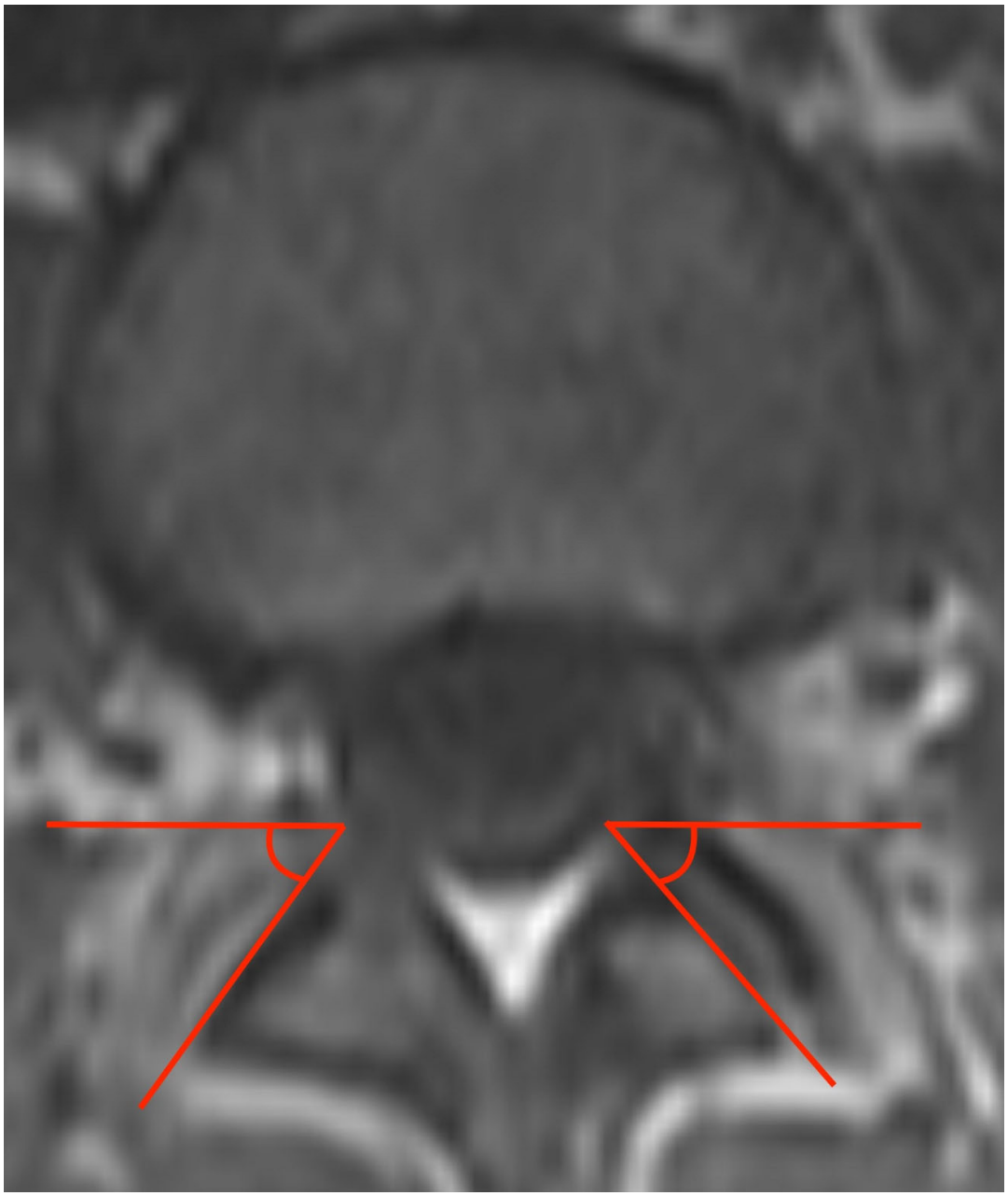

Figure 3: Axial magnetic resonance imaging measurement of the left and right facet joint angle (made by the junction between a line joining the corners of the facet joint and the transverse plane).

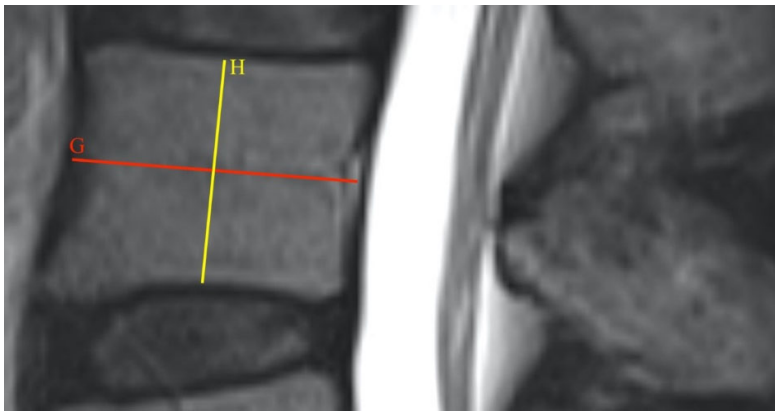

Figure 4: Sagittal magnetic resonance imaging measurements: (G) midline anteroposterior vertebral body diameter; and (H) mid-vertebral body height.

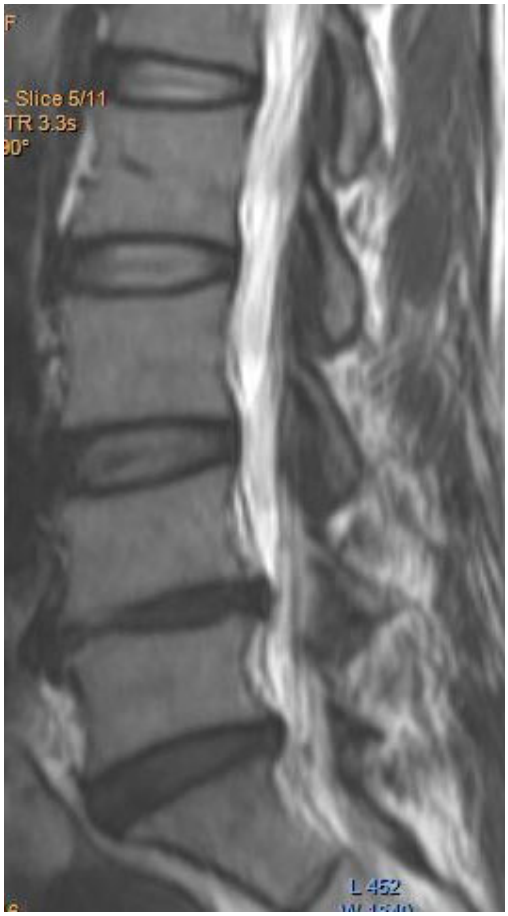

Figure 5: Example of a sagittal magnetic resonance imaging of the L1-S1 discs. The L1-3 discs have no disc herniation and graded Pfirrmann 2. L3-4 has no disc herniation and graded

Pfirrmann 3. L4-5 has disc bulging and graded Pfirrmann 5. L5-S1 has with disc bulging and graded Pfirrmann 4.